



Electric Infrastructure for Goods Transport

Small-scale model of Inductive charging system for long-haul trucks

AUTHORS

Giuseppe Guidi SINTEF Energy Research

2018

Contents

1	Background	V
2	Scaling Criteria	VI
3	Effect of scaling on coil characteristics	VII
3.1	Ideal scaling of electromagnetic quantities	VII
3.2	Effect of number of turns on scaling	VII
4	Selection of scaled model	IX
5	IPT coil design	XI
6	Power conversion system for IPT	XIII
7	Control system for IPT	XIV
8	Realization of IPT prototype	XVI
9	Experimental results	XIX
9.1	Dynamic power transfer	XX
9.2	Bidirectional power transfer	XXIV
10	Conclusion	XXV
11	References	XXVI



1 Background

There is consensus about the benefits of electrifying freight transportation, in terms of drastically reduced emissions of green-house gases, and NO_x as well as in terms of overall energy saving.

Recently, several prototypes of electrified trucks have been built by different manufacturers and many others are being planned. All the models feature an on-board Li-Ion battery as main energy source for the electric motor(s) driving the truck. The size of the battery varies according to the intended payload and expected driving range of the truck, and it is often limited by weight, volume and cost considerations. In light of the quick development of battery technology, it is expected that the first generation of electric trucks will have batteries with capacity in the range of 100–300kWh that must be able to deliver 250–500kW of driving power.

Building infrastructures able to charge such massive batteries in sufficiently short time is a challenge in itself. Having the charging power transferred wirelessly from the road to the cruising vehicle is even more difficult but, thanks to the recent technological advances, practically feasible.

In this context, a reduced scale version of such a dynamic wireless charging system is developed, with multiple aims:

- Show-casing the inductive charging technology;
- Testing design and control methods;
- Demonstrating practical feasibility by accurate scaling-down of key components.

The specifications assumed for the real-scale system are reported in Table 1. The Scania R470 truck tractor model (see Fig. 1) was used as reference for the mechanical dimensions and the motor power, since a suitable scaled model was readily available. At this stage, no detailed study about the optimal amount of on-board energy has been performed, since the results would anyway be very application-dependent.

Table 1 Assumed specifications for a battery-electric truck tractor

Wheel base	3.7 m	Battery Energy	150 kWh
Axle width	2.49 m	Max. Battery Voltage	700 V
Motor Power	350 kW	Charging Power	150 kW (1C)
		Optimal cruising speed	80 km/h



Fig. 1 Truck tractor used as reference for reduced-scale design (picture from "www.favcars.com")

2 Scaling Criteria

Scaling a model depends on what aspects of a particular problem need to be studied, as different physical phenomena follow different scaling laws.

In the case of the dynamic inductive charging system for trucks, the geometrical aspects are deemed most important, in order to demonstrate the expected size of the magnetic components and give an accurate visual image of the system, albeit in scale.

Moreover, the scaled model can be used to run dynamic experiments to see how the power transfer process is affected by the vehicle speed. It is therefore convenient to scale the speed by the same factor as the linear dimensions of the model, while keeping the time invariant.

As a result, a general scaling rule is adopted, where the three spatial dimensions are scaled homogeneously (shapes are preserved), densities are kept invariant, time is kept invariant and, as a result, speed is scaled same as linear dimensions. The resulting scaling factors for basic quantities are reported in Table 2, along with derived scaling for some dependent quantities.

Table 2 Ideal scaling factors for some basic physical quantities

Quantity	Scaling factor
Fundamental scaling choices	
Linear length, m	k_{scale}
Density, kg/m ³	1
Time, s	1
Dependent quantities	
Surface area, m ²	k_{scale}^2
Volume, m ³	k_{scale}^3
Weight, kg	k_{scale}^3
Speed, m/s	k_{scale}
Acceleration, m/s ²	k_{scale}^2
Inertial and gravity forces, Nm	k_{scale}^4
Drag forces, Nm	$k_{scale}^3 - k_{scale}^4$

According to the ideal scaling factors in Table 2, the driving effort should scale with factor close to k_{scale}^4 , resulting in a power requirement for traction that should scale almost with k_{scale}^5 . If the drag force is dominant, then the scaling factor for the traction power may approach k_{scale}^4 . However, this scaling is purely an indication since, while the size can be scaled rather accurately, the assumption of constant densities cannot be guaranteed due to practical constraints. Moreover, due to the low power levels of a scaled model, the influence of stray losses related to friction and inefficiencies of the small-scale power train is expected to be relatively much higher than for the full-scale reference case.

3 Effect of scaling on coil characteristics

3.1 Ideal scaling of electromagnetic quantities

Table 3 shows the electromagnetic characteristics of the main components of the dynamic charging system (road-side and vehicle-side coils), when the scaling criteria specified in the previous section are applied.

Table 3 Scaling factors for some electromagnetic quantities, as result of the selected scaling criteria.

Quantity	Scaling factor
Inductance factors, H/turn ² (*)	k_{scale}
Coil resistance factors, Ω /turn ² (**)	k_{scale}^{-1}
Magnetic coupling coefficient	1
Coil quality factor (***)	1

The table highlights one of the main reason for the selection of the scaling criteria, since it is shown that the electromagnetic properties of the system in terms of achievable coupling and theoretical coil efficiency are unaffected by the adopted scaling process.

Note (*): The inductance factors (or, equivalently, the magnetic reluctances) of the coil are only dependent on the geometry of the system and, under the usual assumption of linearity for the material characteristics, they scale perfectly with the spatial dimensions.

Note (**): The resistance of the coils, assuming a fixed total coil volume, increases with the square of the number of turns N , since the equivalent length of the winding increases linearly with N and the cross-section of each turn decreases linearly with N .

Note (***) : The quality factor of the coils would scale with k_{scale}^2 if the operating frequency is kept constant. However, the operating frequency of a naturally scaled system changes according to k_{scale}^{-2} , as explained in the following. The result is a quality factor independent of scaling.

It is clear that if the windings constituting the ground and vehicle coils are perfectly scaled down, meaning that the number of turns (and shape) is preserved, the same current density and isolation stress (same electric field) in the coil windings are achieved by scaling the coil current by k_{scale}^2 and the coil voltage by k_{scale} . It can be demonstrated that those constraints can only be satisfied if the resonant frequency of the coils is scaled according to k_{scale}^{-2} , meaning that reduced-scale models will have to be operated at higher frequency.

With this natural scaling, the maximum power of the IPT system scales with k_{scale}^3 .

One consequence of the above is that the power capability of the scaled-down IPT system can easily exceed the effective power required for driving the small-scale model, since ideally the required traction power scales at least as k_{scale}^4 .

3.2 Effect of number of turns on scaling

A slight modification to the perfect scaling procedure described above consists in changing the number of turns of both road-side and vehicle-side coils while keeping the turn ratio unchanged. This keeps the characteristics of the electromagnetic coupling (and therefore those of the power transfer process) unchanged, with the only effect of changing the ratio between current and voltages on both side of the inductive link.

It should be noted that if only one side is changed or, in general, the turn ratio is made different between real-scale model and scaled model, the characteristics of the system are no longer identical. In particular, the theoretical efficiency of the power transfer may change and the normalized impedances of the two systems have different characteristics.

4 Selection of scaled model

The scaling factor has been mainly decided according to availability of suitable off-the-shelf models of the vehicle. It has therefore been decided to use a radio-controlled model from Tamiya as shown in Fig. 2.

This model is a rather accurate replica of the original truck on a 1:14 scale, which gives a reasonable size for the implementation of the dynamic IPT system that can serve as both showcase and as experimental test bench for validation of design and control methods.

Another advantage of the Tamiya model is that it comes equipped with remote-controllable, electrical servo-drives supplied by an on-board battery. That simplifies the implementation, as only the dynamic wireless system components must be designed and developed to achieve full functionality.

The main specifications of the electrical drive system on-board the truck model are reported in Table 4.



Fig. 2 Tamiya 1:14 RC-model of Scania R470-Highline truck tractor and trailer used for the project.

Model scale	$k_{scale} = 1/14$
On-board battery (*)	Li-Po, 7.4V, 6500 mAh
RC servo motors	Driving (fwd-rev) Shifting (3 gears) Steering

Table 4 Main electrical specifications of the truck model.

Note (*): The original NiMH battery sold with the model has been replaced by a more suitable LiPo battery that can achieve continuous charge at high current, as required by the application.

Combining data of Table 1 and Table 4, following the natural scaling rules for current, voltage and frequency results in:

$$\begin{aligned}
 P_{chg,out,ideal} &= 150 \text{ kW} / 14^3 = 55 \text{ W} \\
 V_{chg,out,dc,ideal} &= 700 \text{ V} / 14 = 50 \text{ V} \\
 I_{chg,out,dc,ideal} &= 1.1 \text{ A} \\
 f_{0,ideal} &= f_{0,FS} \cdot 14^2
 \end{aligned} \tag{1.1}$$

The actual battery of the model has much lower voltage than the one calculated following the natural scaling. In order to avoid the need for an additional dc/dc conversion stage, the degree of freedom of the number of turns can be used to adapt the voltage levels, resulting in the following terminal specifications for the scaled charger:

$$\begin{aligned}
 V_{chg,out,dc,ideal} &= 7.4V = 0.15 \cdot V_{chg,out,dc,ideal} \\
 I_{chg,out,dc,ideal} &= \frac{1.1A}{0.15} \approx 7.3A
 \end{aligned}
 \tag{1.2}$$

The biggest problem of the scale-down process is related to the operating frequency of the IPT system. In fact, the resonant frequency of the full-scale system will be most likely dictated by strict regulations. At present, two frequency windows seem the most likely candidate, centred at 20 kHz and 85 kHz respectively.

According to (1.1) the scaled system would have to be operated at 3.9 MHz or 16.6 MHz, respectively. While theoretically possible, operation at such high frequencies is extremely challenging and goes well beyond the state-of-the-art, especially if the system has to be continuously controlled to adapt to the changes resulting from the vehicle motion.

For this reason, it has been decided to deviate from the perfect scaling procedure and to design the small-scale model for an operating frequency similar to the target frequency of the full-scale one:

$$f_0 = f_{0,FS} = 85kHz = \frac{f_{0,ideal}}{14^2}
 \tag{1.3}$$

Unfortunately, the consequence of such design choice is that **the model will not be an exact small-scale replica of the full-scale one**, unless the latter can be operated at the unlikely frequency of 850 Hz.

On the good side, raising the operating frequency of the full-scale system implies reducing the size of it and/or raising the operating voltages. This will of course increase power density, challenging cooling and isolation, but is expected to result in more compact and more efficient systems.

5 IPT coil design

In order to reduce complexity, the simplest possible coil configuration has been selected, consisting of planar unipolar coils for both the road-side and the vehicle-side, as shown in Fig. 3

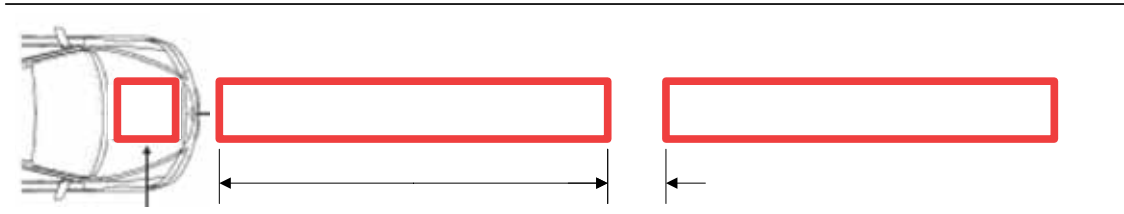


Fig. 3 General view of the layout of single coil road-sections for inductive power transfer to a moving vehicle

The coils are designed according to the specifications in Table 5, following from the considerations of the previous sections and taking into account the space available on the truck model.

Note that the length of the road-side coil along the traveling direction has been set to an equivalent of 8.0 m in full-scale. This is believed to be a reasonable length for the coil sections of an inductive road, compromising between efficiency, utilization factor and infrastructure cost. Different lengths are of course possible and segments of different lengths can easily coexist on the same road, as long as the associated capacitor banks are tuned to achieve the same resonant frequency for all the segments.

Table 5 Specifications of the 1:14 scaled model of dynamic inductive power transfer system.
Red text in parenthesis indicates equivalent quantities in full-scale.

Nominal power, P_o	55 W (150 kW)
I/O voltages, $V_{dc,in}$, $V_{dc,out}$	12.0 V, 7.4 V
Effective power transfer distance (ground clearance + road-coil burying depth)	21 mm (30 cm)
Operating frequency	85 kHz
Road-side coil MAX planar dimensions	570 x100 mm (8.0 x1.4 m)
On-board coil MAX planar dimensions	100 x100 mm (1.4 x1.4 m)

Series-Series (SS) capacitive compensation has been selected, due to its simplicity and to the excellent characteristics in terms of relative insensitivity to changes in coupling. The latter is particularly important in dynamic charging systems where the relative position of the coils is changing rapidly. An additional positive aspect of SS-compensated system is their symmetry, allowing for easier implementation of bidirectional power transfer, if required.

The criteria described in [1], [2] have been used to design the coils. Analytical calculations have been checked by FEM simulations executed in Comsol, before proceeding to the actual realization of the model. Results of the FEM analysis (see Fig. 4) have confirmed the validity of the underlying analytical model and thus the feasibility of the system.

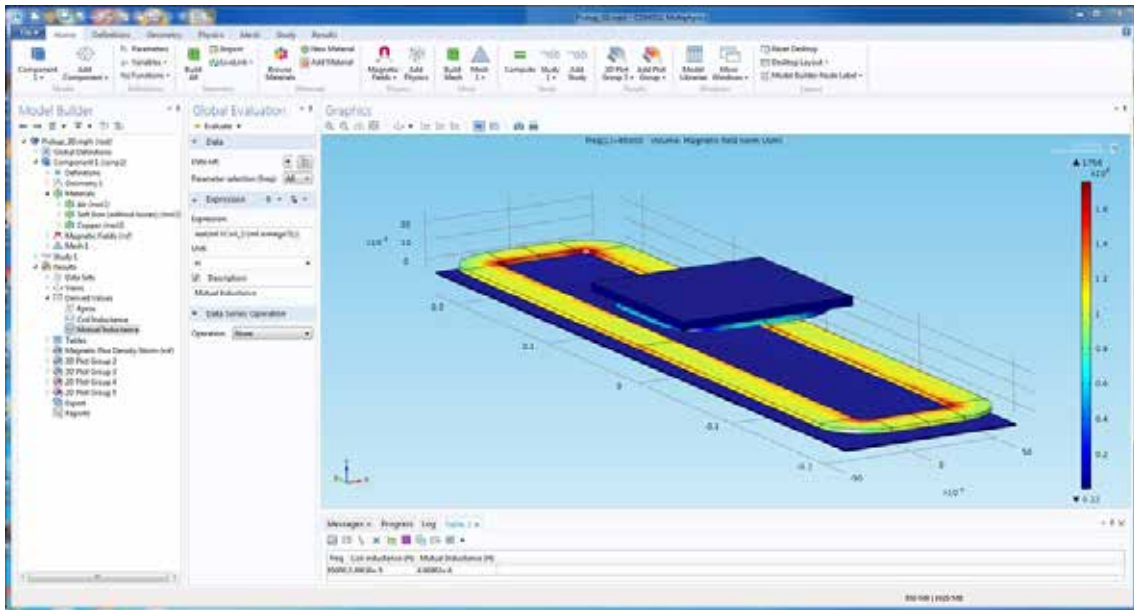


Fig. 4 Example of electromagnetic field calculation for the model, using the FEM software Comsol.

6 Power conversion system for IPT

A system for transferring energy via inductive coupling from the road to a vehicle must include the following power conversion stages:

- Rectification of the 50/60 Hz 3-phase main supply;
- Conversion of the dc power into a high frequency ac power that is sent through the inductive link;
- Controlled rectification of the high-frequency ac power into a dc power that is suitable for battery charging.

Intermediate conversion stages are sometimes inserted to improve controllability or to optimize efficiency of the overall system.

The system in Fig. 5 is used in the prototype. The first rectification stage (50Hz to dc) is not shown, since any conventional rectification technique can be used.

Advantages of the selected topology are:

- Minimum number of converters; only two H-bridges are used, one on each side of the link.
- Minimum number of reactive components; only the coils and the series-resonant capacitors are needed, simplifying the system and minimizing volume/weight.
- Perfect symmetry, making the system ideal for dynamic, bidirectional power transfer.

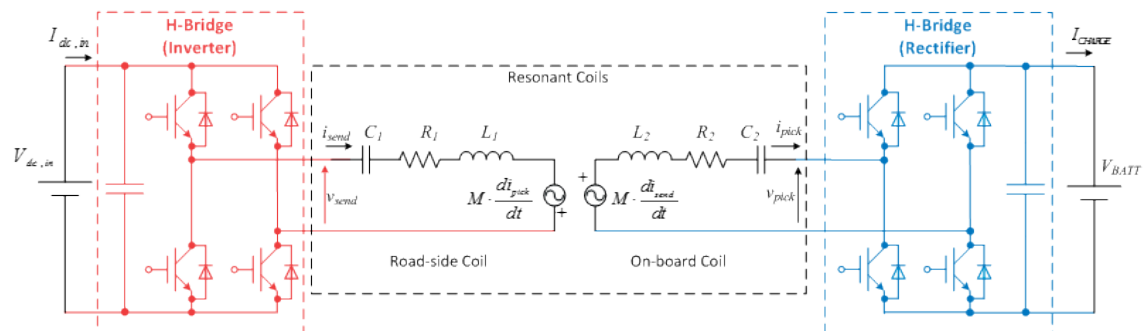


Fig. 5 Overview of the power conversion topology used in the IPT prototype

On most systems, the on-board rectifier (the blue part in the figure) is implemented as a double-stage conversion system consisting of a passive diode bridge followed by a dc-dc conversion stage. Although apparently more complex, this solution may lead to higher efficiency especially at partial load and is in general easier to control, since synchronous operation of the rectifier is not required. However, bidirectional power flow cannot be achieved.

7 Control system for IPT

The most important feature of a dynamic charging system is the ability to strictly control the charging/discharging current of the battery, rejecting the disturbances due to the motion of the vehicle. In addition, any practical implementation must be robust against unexpected events like faults, grid failures, etc.

The following control paradigms are used in the prototype:

- Battery current is directly controlled by the on-board system and is independent of the road-side supply. The on-board BMS decides the optimal charging level according to driving conditions, SOC, etc. The on-board converter regulates the power flow accordingly and protect itself in case of unexpected events.
- The road-side transmitter is activated according to external vehicle-detection logic, but self-protects in case of unexpected events, avoiding for instance excessive current to flow if the vehicle suddenly ceases to absorb power.
- No communication between road-side and vehicle-side converter controllers is needed for the main power flow process. Slow communication will normally be in place and can be used for optimizing the efficiency of the transfer process, but safe system operation does not depend on it.

Basic implementation of the control strategy is summarized by Fig. 6 and Fig. 7, where the sequencing and the regulation algorithms for the road-side and the vehicle-side are show, respectively.

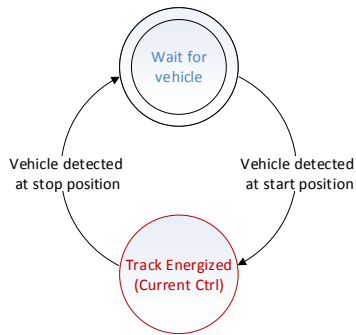
The charging system on-board is normally in an active stand-by state, where the coil is short-circuited and, if there is no energized track in the vicinity, no current flows. As soon as the vehicle moves onto an energized track, current starts to flow in the short-circuited coil and the on-board PLL can lock. At this point, current control is enabled and the on-board H-bridge starts controlling the voltage to regulate the charging current to the desired value. If, at any moment, the vehicle moves away from the energized track, the current in the on-board coil decays and the system goes back into the active stand-by state.

The road-side coil (see Fig. 6) is energized as soon as an approaching vehicle is detected at a specific position. Detection method is application dependent and can in itself be the object of research activity.

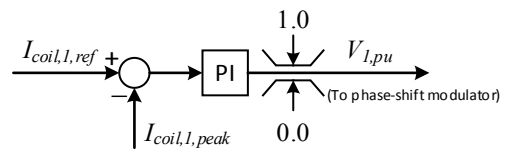
When energized, the road-side converter tries to control the current of the SS-compensated coil to a preset level corresponding to the track current needed to charge the on-board battery under worst-case coupling conditions. Typically, when the vehicle appears on the track and starts charging the on-board battery, the impedance of the road-coil will naturally raise, bringing the track current to a value that is lower than what the road-side regulator is trying to inject. As a consequence, the road-side H-bridge will automatically operate in square-wave voltage mode, with track-side current solely determined by the charging power required by the vehicle.

If, at any time during the charging process, the vehicle leaves the track or stops charging the on-board battery, the impedance at the terminals of the road-side converter decreases and the roadside regulator takes over and limits the current to the pre-set limit. It is therefore perfectly safe, as far as the operation of the track coil and the associated converter are concerned, to keep the track energized at all times, with or without charging vehicles on it. The only issues would then be unnecessary losses due to the circulating current (mostly reactive power supplied by the H-bridge to the resonant track) and possibly higher radiated emissions due to the absence of the shielding action of the vehicle.

A more detailed description of the control paradigms is given in [3].

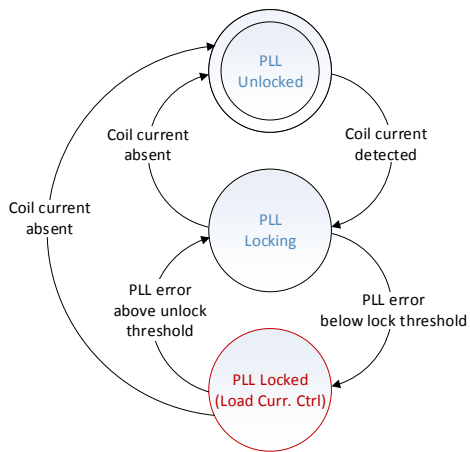


(a) Road-coil energization strategy

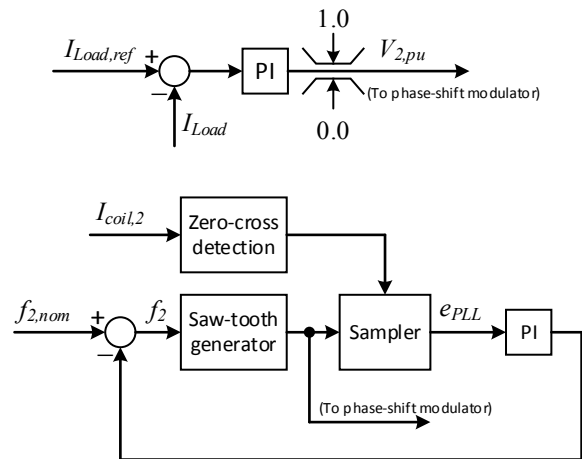


(b) Structure of road-coil current regulator

Fig. 6 Basic control strategy for road-side IPT operation



(a) Road-coil energization strategy



(b) Structure of road-coil current regulator and associated PLL

Fig. 7 Basic control strategy for vehicle-side IPT operation

8 Realization of IPT prototype

Table 6 Measured characteristics of the coils

Road-side coil	
Planar dimensions	570 x100 mm (8.0 x1.4 m)
Self-inductance (with no pick-up), L_1 ,	36.7 μ H
Resonance frequency (with no pick-up)	74 kHz
Measured resistance (at 75 kHz)	128 m Ω ,
Vehicle-side coil	
Planar dimensions	100 x100 mm (1.4 x1.4 m)
Self-inductance (above road-side coil), L_2 ,	8.3 μ H
Resonance frequency (above road-side coil)	78 kHz
Measured resistance (at 75 kHz)	65 m Ω ,
Coupling factor with gap = 22 mm, precise alignment	
Pickup in the middle of road coil (min. coupling)	0.16
Pickup close to the end of road coil (max. coupling)	0.18



Fig. 8 Assembly of the on-board coil and associated resonant capacitors on the truck model.

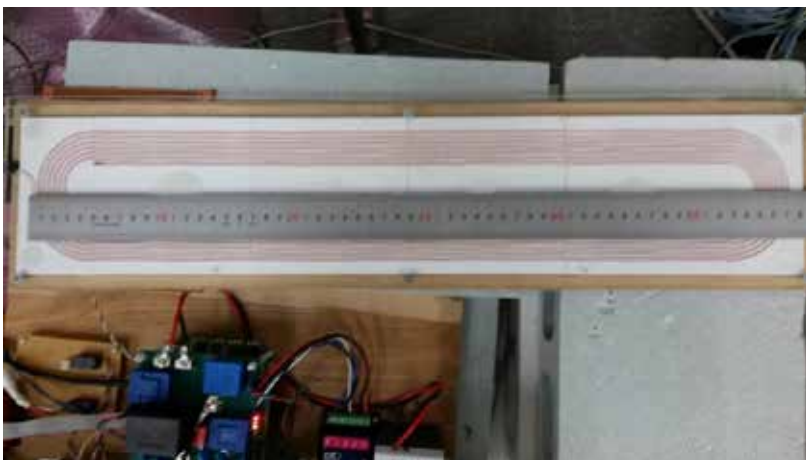


Fig. 9 Assembly of the road coil.

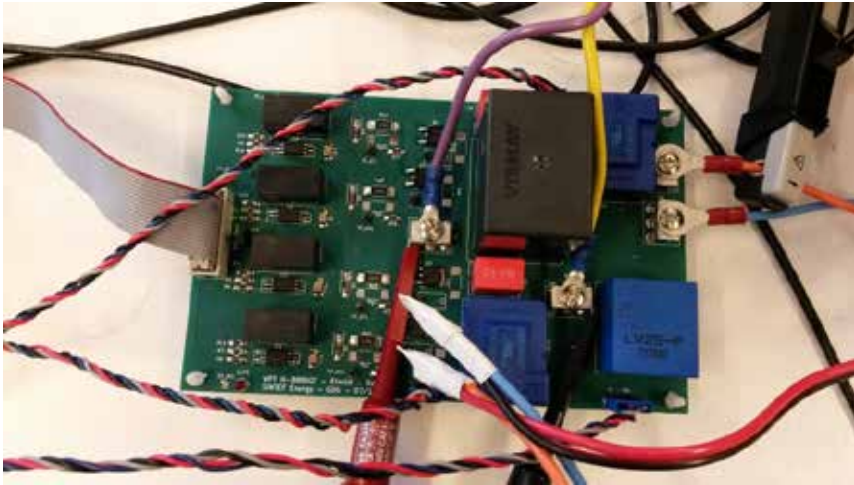


Fig. 10 ElnGO Power board with the MOSFET-based H-Bridge, gate drivers, voltage/current sensors.



Fig. 11 On-board power conversion system for the IPT, including battery, H-bridge and controls.

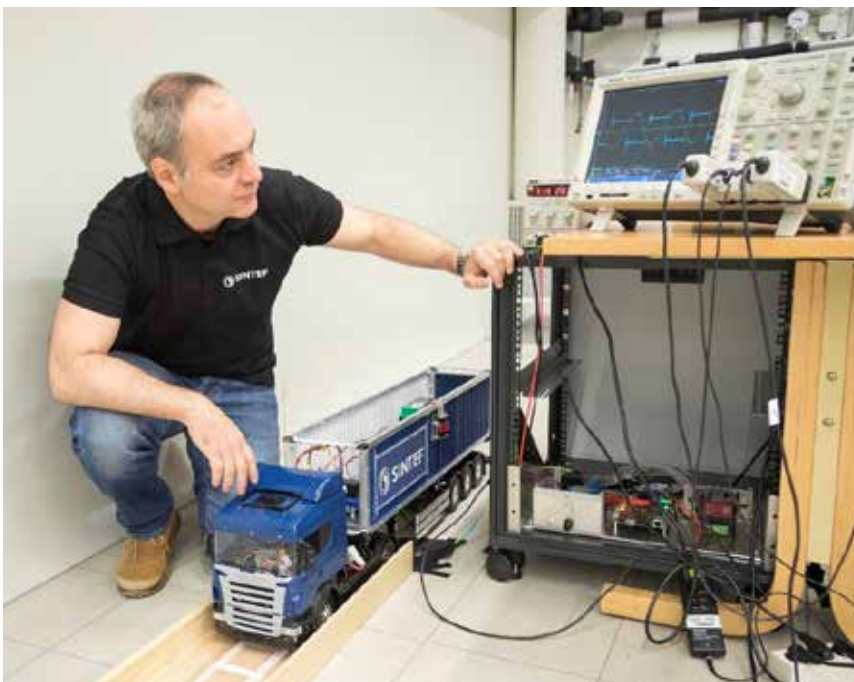


Fig. 12 Static test of the complete IPT prototype



Fig. 13 The radio-controlled truck model running on the on-road coil, demonstrating the dynamic inductive power transfer

9 Experimental results

Apart from the concept demonstration, consisting in showing the truck model charging the on-board battery while running, more detailed experimental investigation has been carried out.

In particular, the dynamic power transfer process has been analysed using the facilities available at Hori-Fujimoto laboratory at The University of Tokyo, Japan, during a 6-weeks long research stay supported by an internal project at SINTEF Energy Research.

The coils fabricated for the truck prototype have been mounted on the servo-controlled sliding rail shown in Fig. 14, and data related to the power transfer process has been recorder in strictly-controlled laboratory conditions. Results have been published in a peer-reviewed paper for an IEEE conference [3].

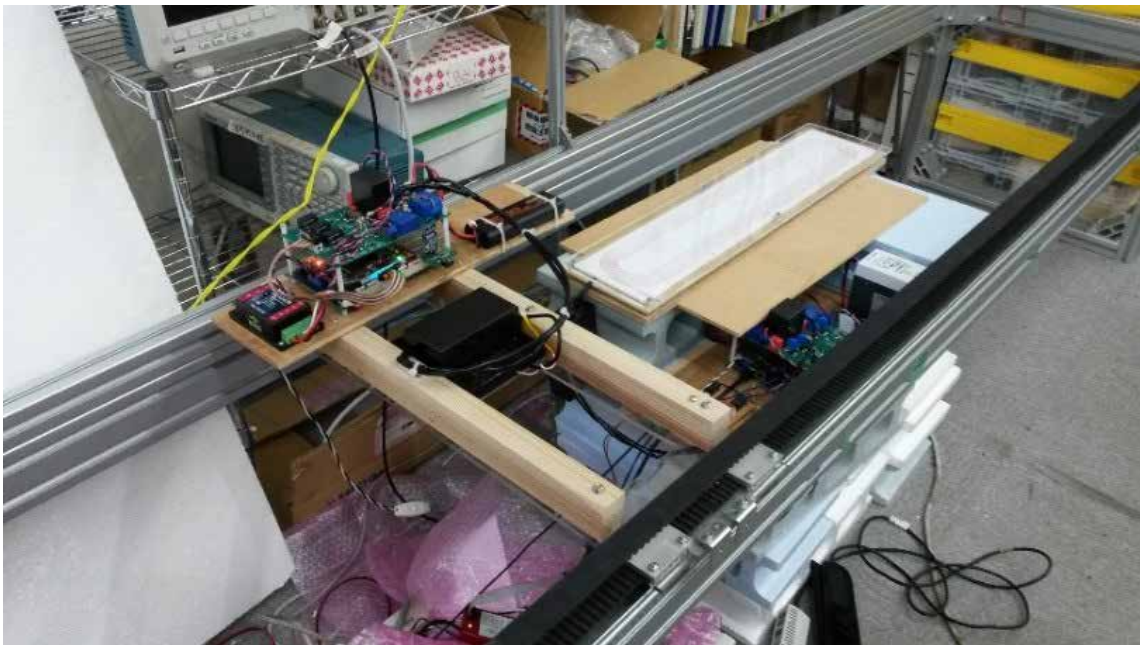


Fig. 14 Servo-controlled rail used for dynamic power transfer experiments at the University of Tokyo, Kashiwa campus.

9.1 Dynamic power transfer

Operation strategies are proposed for activating the coils in order to achieve the best possible efficiency and without overloading the converters.

Some of the key data is reported in the following figures and in Table 7. Detailed description of the operation and corresponding evaluation of more extensive results can be found in [3].

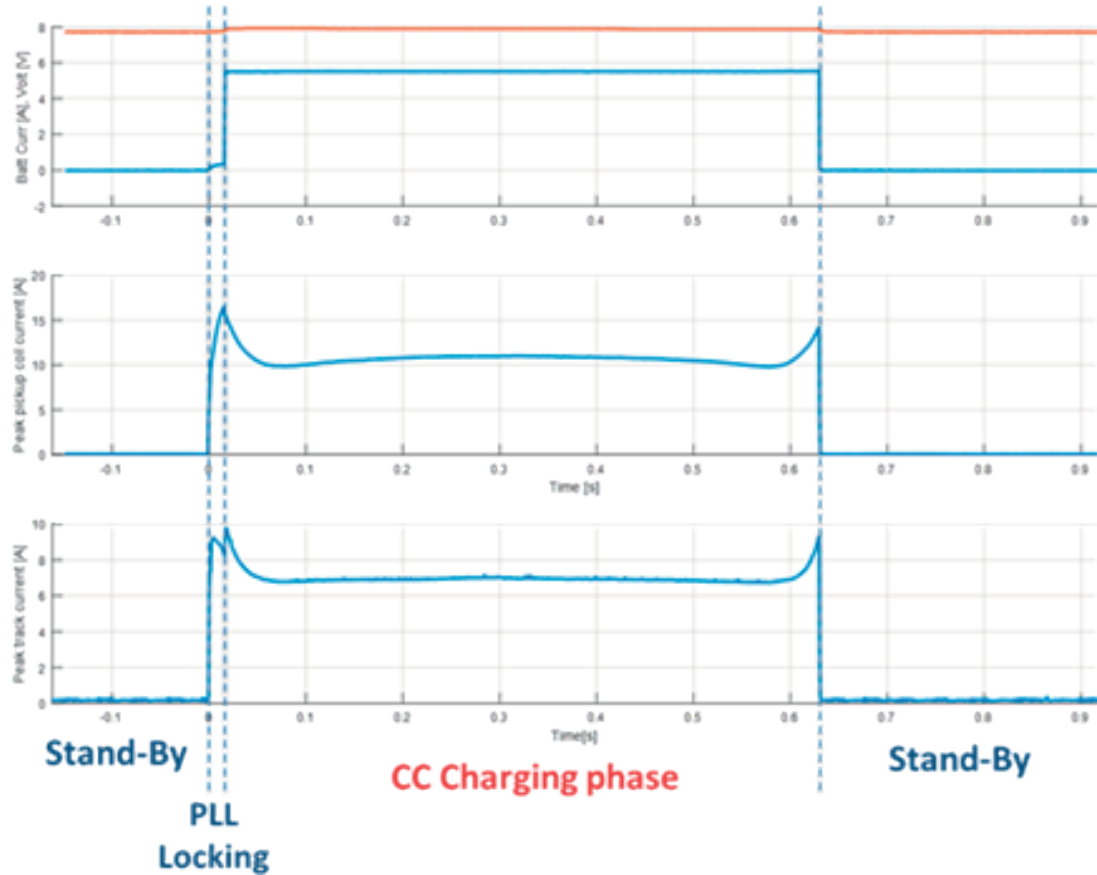


Fig. 15 Experimental results: IPT process at 845 mm/s (equivalent to 42 km/h in full-scale) as function of time. From top to bottom: On-board battery current/voltage, On-board coil current (peak envelope), Road coil current (peak envelope).

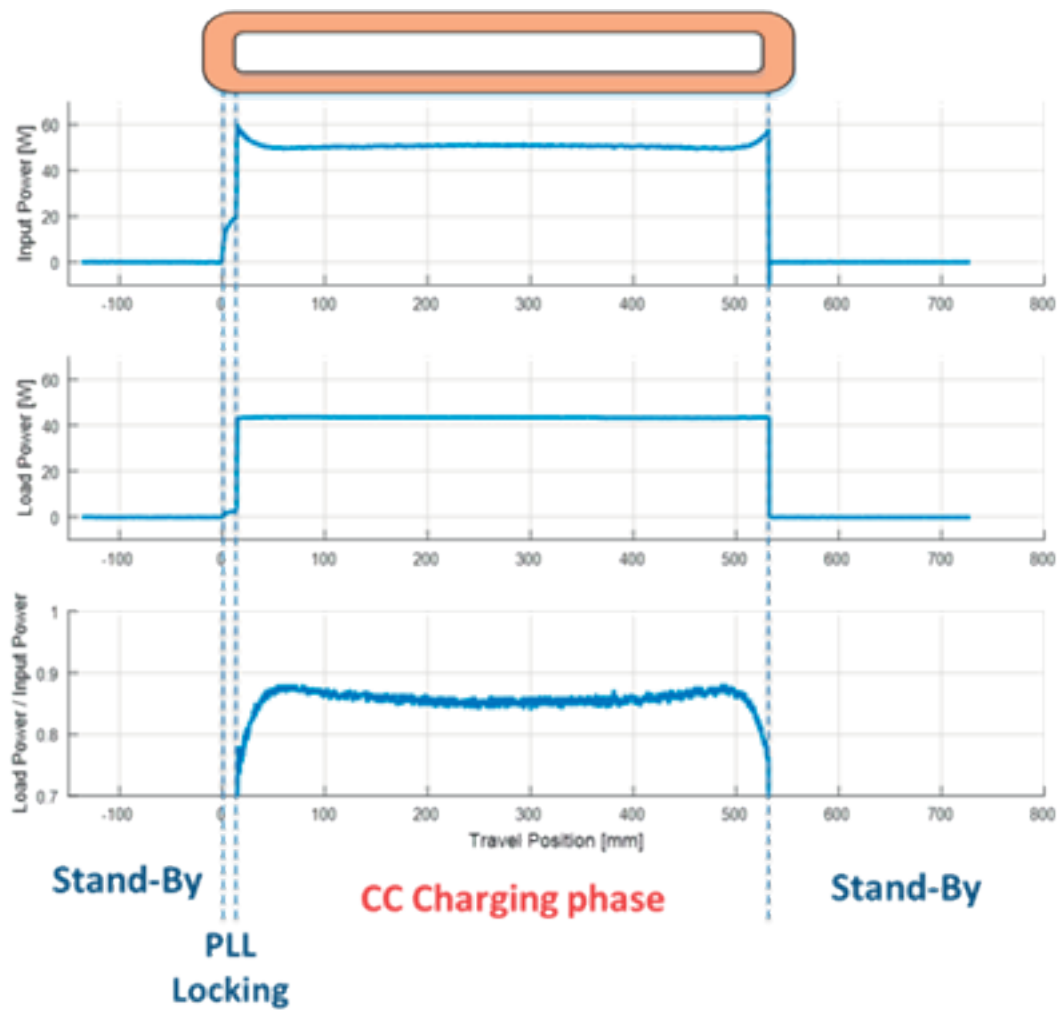


Fig. 16 Experimental results: IPT process at 845 mm/s (equivalent to 42 km/h in full-scale) as function of relative position. From top to bottom: Input power (to road converter), Output power (to battery), Instantaneous power ratio (efficiency, in case of negligible storage).

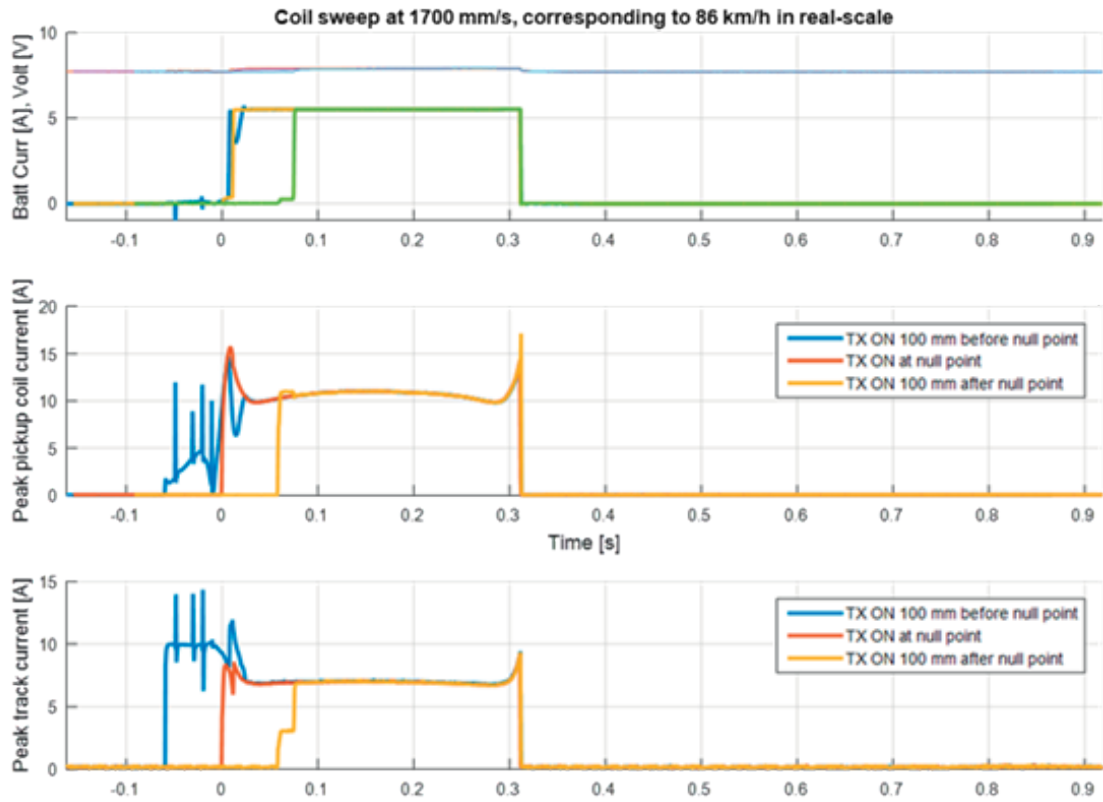


Fig. 17 Experimental results: IPT process at 1700 mm/s (equivalent to 86 km/h in full-scale) as function of time for different energization instants of the road-coil. From top to bottom: On-board battery current/voltage, On-board coil current (peak envelope), Road coil current (peak envelope).

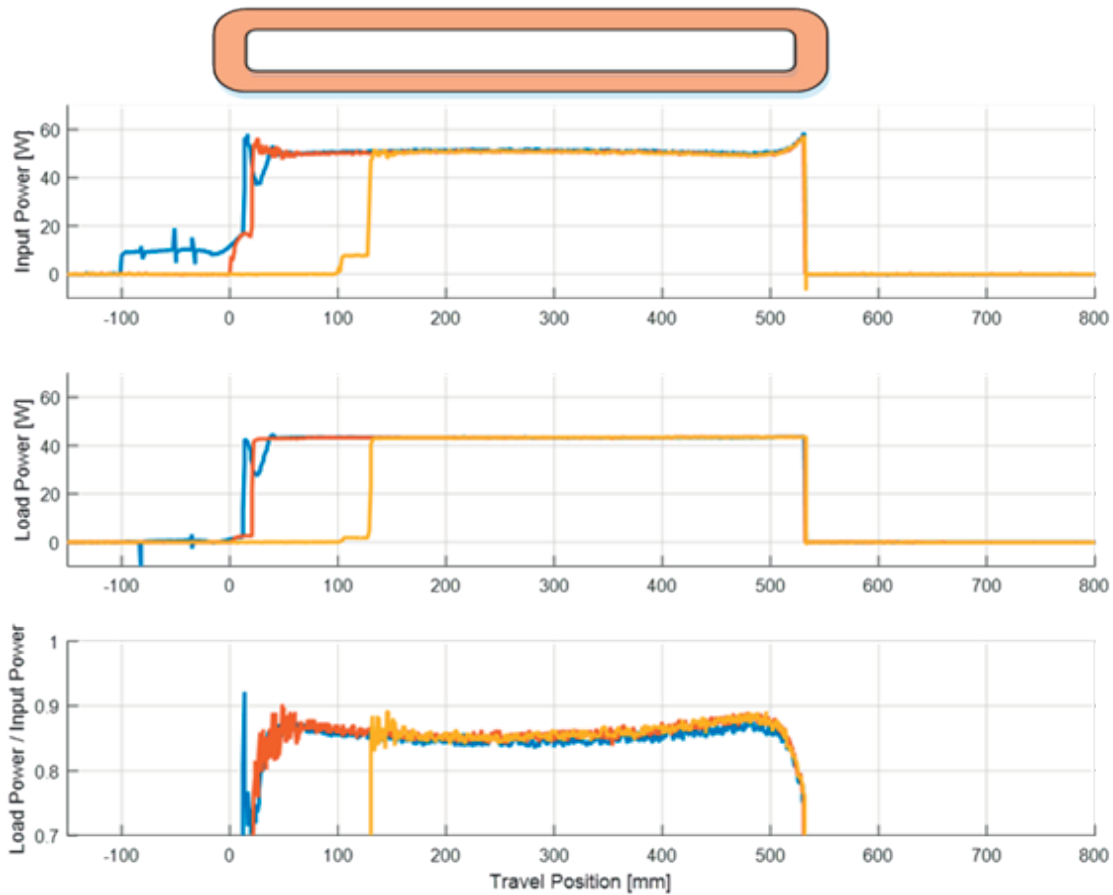


Fig. 18 Experimental results: IPT process at 1700 mm/s (equivalent to 86 km/h in full-scale) as function of relative position for different energization instants of the road-coil. From top to bottom: Input power (to road converter), Output power (to battery), Instantaneous power ratio (efficiency, in case of negligible storage).

845 mm/s (42.5 km/h)		
$E_{2_{-100}} = 20.3 \text{ J}$	$\eta = 0.80$	$P_{AV} = 25.5 \text{ W}$
$E_{2_0} = 20.4 \text{ J}$	$\eta = 0.82$	$P_{AV} = 25.7 \text{ W}$
$E_{2_{100}} = 17.3 \text{ J}$	$\eta = 0.83$	$P_{AV} = 21.8 \text{ W}$
1700 mm/s (86 km/h)		
$E_{2_{-100}} = 9.9 \text{ J}$	$\eta = 0.80$	$P_{AV} = 25.2 \text{ W}$
$E_{2_0} = 9.7 \text{ J}$	$\eta = 0.82$	$P_{AV} = 24.7 \text{ W}$
$E_{2_{100}} = 7.7 \text{ J}$	$\eta = 0.82$	$P_{AV} = 19.6 \text{ W}$

Table 7 Energy transferred and overall transfer efficiency as function of vehicle speed and relative position at which the road-coil is energized.

9.2 Bidirectional power transfer

The possibility of reverting the power flow has also been demonstrated. Indeed, extremely fast power reversal has been achieved by using the proposed controllers. These results are still unpublished but will be presented in a suitable peer-reviewed international conference.

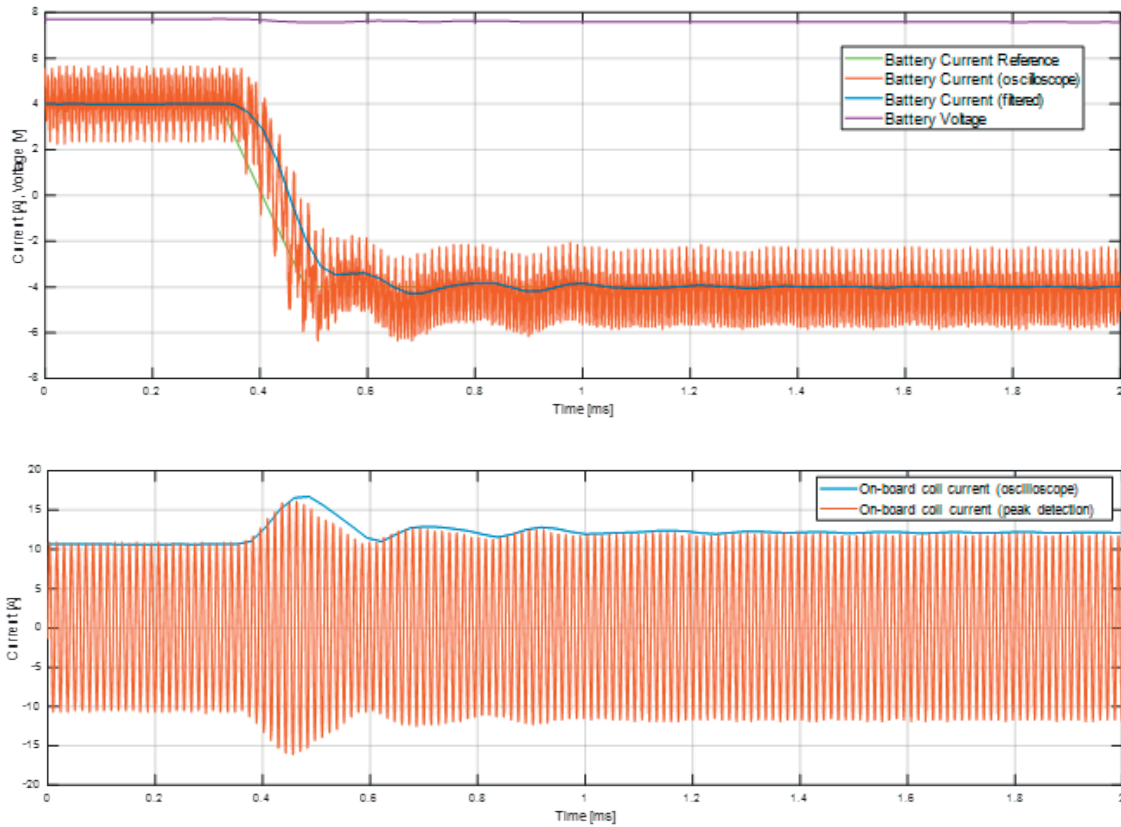


Fig. 19 Experimental results: Quick reversal of power flow through the IPT link. From 1C charge to 1C discharge of the on-board battery in about 0.2 ms.

10 Conclusion

A model in scale 1:14 of a dynamic contactless power transfer system for long-haul trucks has been built and tested.

The demonstrator is built according to geometric scaling of the real system, giving a rather accurate image of the full-scale implementation, although not all the characteristics of the system can be properly scaled. It is expected that the full-scale system can achieve higher power density and efficiency compared to the 1:14 model, whose peak transfer efficiency has been measured to be around 88%. The know-how developed in previous projects has been used for the design of the coils and converters.

New control algorithms have been developed to operate the overall system, with the aim of maximizing transfer efficiency while minimizing material use.

The model has been tested in strictly-controlled laboratory environment and data has been published in one peer-reviewed international conference. More publications are planned in the near future.

11 References

- [1] G. Guidi, "An apparatus and a method for wireless transmission of power between DC Voltage sources," Norwegian Patent application 20150087, January 2015
- [2] G. Guidi, J. A. Suul, "Minimizing Converter Requirements of Inductive Power Transfer Systems with Constant Voltage Load and Variable Coupling Conditions," in IEEE Transactions on Industrial Electronics, Vol. 63, No. 11, November 2016, pp. 6835-6844
- [3] G. Guidi, J. A. Suul, "Transient Control of Dynamic Inductive EV Charging and Impact on Energy Efficiency when Passing a Roadside Coil Section", in Proc. IEEE PELS Workshop on Emerging Technologies: Wireless Power (WoW 2018), Montreal, Canada, June 3-7 2018, 7 pp..



With funding from
The Research Council of Norway